Electromagnetic Radiation Driven Phase Transition in Silver Telluride-Iron Oxide and Iron Telluride Nano-Composites

Yang Bao [1,3], Wei Zheng [2], Praveen Gurrala [3], Biao Xu [4], Jiming Song [3], and Yue Wu [2]

[1] College of Electronic and Optical Engineering
Nanjing University of Posts and Telecommunications, Nanjing, Jiangsu 210023, China
brianbao@njupt.edu.cn

[2] Department of Chemical and Biological Engineering
Iowa State University, Ames, IA 50011, USA
zhengwei@iastate.edu; yuewu@iastate.edu

[3] Department of Electrical and Computer Engineering
Iowa State University, Ames, IA 50011, USA
praveeng@iastate.edu; jisong@iastate.edu

[4] School of Chemical Engineering
Nanjing University of Science and Technology, Nanjing, Jiangsu 210094, China
xubiao@njust.edu.cn

Abstract ─ Temperature-dependent switchability of electrical property has drawn a lot of attention recently. In this article, electromagnetic (EM) radiation is used to induce temperature change in silver telluride and iron telluride nanostructures, which can be potentially used to trigger electrical property changes in them. Due to the low EM absorptivity of silver telluride nanowire, heating it via EM fields is very challenging. To enhance its EM absorptivity, various percentages (by mass) of iron oxide powder are mixed into it. It is verified that, similar to pure silver telluride, the mixture also exhibits a rapid change in electrical conductivity within a certain temperature range. The experiment is designed to characterize the EM absorptivity of three such mixtures with different percentage compositions and an iron telluride nanodisk in the X-band frequency range (8 to 12 GHz). The temperature increase induced by the absorbed EM energy will lead to the rapid change of electrical conductivity by α -type to β -type phase transition in silver telluride and p-type to n-type transition in iron telluride, which can be potentially used to develop EM sensors for applications in communication technology.

Index Terms ─ Electrical switchability, electromagnetic radiation absorption, EM sensor, nano-composites.

I. INTRODUCTION

With the rapid development of wireless communication, the increasing usage of electromagnetic devices results in serious electromagnetic interference (EMI) and electromagnetic compatibility (EMC) problems [1-4]. More seriously, the high density of electromagnetic (EM) radiation caused by wireless communication has been confirmed to have a great effect on the health and safety of humans, such as sleep disturbance, headache, nausea, visual disorders, respiratory problems, and nervous excitation [5].

In consideration of the pollution and threat from EM radiation, many ideas have been proposed to prevent the radiation from being harmful to the humans and communities. EM sensors or switches have since come out. There are some sensors or switches based on amorphous semiconductor [6], superconductor [7], and high-pressure gas arresters [8]. However, semiconductor-based switches have a limited number of operations when protecting circuits against high voltage transients, superconductors require low-temperature cooling, and gas arresters have complicated design with relatively large size [9]. After that, in recent years, significant progress has been achieved in microwave cryogenic electronics operating at liquid nitrogen temperatures [10]. Symmetrical thin-film switches based on current-induced phase transitions from superconductor to normal state [11], and polycrystalline manganite films exhibiting the "electro-resistance" effect [12] were proposed. However, the high speed of operation of these sensors is always accompanied with energy focusing in narrow channels of the film and damage to the protector [10]. To overcome the drawbacks mentioned above, the potential use of silver telluride and iron telluride

Submitted On: November 4, 2019
Accepted On: April 18, 2020

nanostructures in EM sensors are considered, where Joule heating induced by the EM energy absorbed by these materials triggers rapid electrical property changes.

In this article, silver telluride nanowire, which has low EM absorptivity, is blended with iron oxide powder, which has higher ability to absorb EM radiation energy and subsequently convert it into heat or other forms of internal energy [13-17], to improve the mixtures' EM absorptivity while keeping the feature of rapid electrical property changes [18-26]. The EM absorption properties of three mixture samples with different percentages of silver telluride nanowire and iron oxide powder, and a nanodisk made of iron telluride are measured in X band, which is in great demand [27-30]. The good EM absorption properties of these materials can lead to increase in their temperature in environments with high EM radiation. This will eventually cause the rapid change of the electrical conductivity by α -type to β -type phase transition [31-32] in silver telluride and p-type to n-type transition [33-34] in iron telluride, which can be potentially applied to develop EM sensors. The remainder of this paper is organized as follows. Section II describes the experimental details. Section III shows the results and discussion. Finally, the conclusion is drawn in Section IV.

II. EXPERIMENTAL DETAILS

All chemicals are used as received without further purification. Tellurium dioxide (≥99.99%), polyvinylpyrrolidone (PVP, MW~ 40,000), potassium hydroxide, (KOH, ≥90%), hydrazine monohydrate (N_2H_4•H_2O, 78%~82%), and iron oxide (Fe_3O_4, ≥99.99%, 325 mesh) were purchased from Sigma Aldrich, while silver nitrate ($AgNO_3$, ≥99.9%), ethylene glycol (EG, ≥99%) and ethanol (≥95%) were purchased from VWR.

For the synthesis of Ag_2Te_2xAg nanowires, the procedure from our previous publication was followed exactly [32]. Firstly, 9.576 g TeO_2, 12 g PVP, 44.484 g KOH, and 600 ml EG were added to a 1 L glass reactor with magnetic stirring initiated for continuous mixing. The glass reactor was heated to 120°C and 20 ml N_2H_4•H_2O was rapidly injected into the reactor. Here the TeO2 served as a precursor for Tellurium, N_2H_4•H_2O was a reductant to provide electrons with Te, while KOH was added to tune the pH of the solution and the reaction rate. The temperature was maintained at 120°C for 1 hour under nitrogen gas protection. Then, the reaction was stopped and cooled down to room temperature naturally. The tellurium nanowire was washed three times with deionized (DI) water and re-dispersed in 800 ml EG in a 2 L beaker for Ag_2Te synthesis. Alongside, 40.769 g $AgNO_3$ was dissolved in 200 ml EG. Then, the $AgNO_3$/EG solution was added into the 2 L beaker and stirred at room temperature for 2 hours for the conversion from Te into Ag_2Te. In this process, AgNO3 was reduced to metallic Ag and then combined with Te to yield Ag2Te. The as-synthesized Ag_2Te_2xAg nanowires were centrifuged two times with deionized water and washed in an ethanol solution (12.5% of N_2H_4•H_2O) for 24 hours to remove the surfactant. The mixture was then washed twice with ethanol and vacuum-dried.

Ag_2Te-Fe_3O_4 composite sintering: The Ag_2Te nanowires was grounded into loose powder and griddled by a 325-mesh sieve in a nitrogen-filled glovebox. Ag_2Te and Fe_3O_4 powder were mixed evenly by mortar and loaded into graphite die for spark plasma sintering (SPS). The sintering condition was under 40 MPa at 850°C for 5 minutes and then cooled down to room temperature naturally [33].

The EM absorption property was measured using a programmable vector network analyzer (VNA, Agilent E8364) with calibration kit (Agilent 85052D) and cables (GORE Microwave). The samples were placed inside an X band waveguide (Aircom Microwave) to measure the S parameters.

III. RESULTS AND DISCUSSION

The Ag_2Te is analyzed by using X-ray diffraction (XRD) and transmission electron microscopy (TEM). The XRD result, Fig. 1 (a), shows that our synthesized Ag_2Te can be indexed as pure monoclinic phase silver telluride (red lines: JCPDS # 34-1042). Figure 1 (b) is the low-magnification TEM image of Ag_2Te and Fig. 1 (c) is the high-resolution TEM (HRTEM) image of Ag_2Te with its fast Fourier transform (FFT) image. The synthesized Ag_2Te is further proved to be the same monoclinic phase of Ag_2Te (space group is 13).

This large-scale solution-synthesis method enables us to sinter several Ag_2Te - Fe_3O_4 composite disks with 1 cm diameter by Spark Plasma Sintering (SPS) and investigate the electrical properties of the resulting mixtures. Figure 2 (a) is the XRD results of Ag_2Te - Fe_3O_4 composites, where all percentages are by weight. There are both silver telluride peaks (JDCPS #34-1042) and iron oxide peaks (JCPDS #19-0692) in all three composite disks. With increasing Ag2Te weight percent, Ag2Te peaks increase while Fe3O4 peaks decrease. The Seebeck coefficient of Ag_2Te - Fe_3O_4 composites has been measured from 40°C to 220°C and is shown in Fig. 2 (b). All these three samples have negative Seebeck coefficient values during the test temperature range which indicate they are n-type semiconductors.

For 25% Ag_2Te-75% Fe_3O_4 and 50% Ag_2Te-50% Fe_3O_4 samples, the absolute Seebeck coefficient increases with temperature. However, the absolute Seebeck coefficient of 75% Ag_2Te -25% Fe_3O_4 decreases first then increases after 125°C. Figure 2 (c) is the electrical conductivity of Ag_2Te - Fe_3O_4 composites. The 25% Ag_2Te -75% Fe_3O_4 sample has the highest electrical conductivity with the value between 140 S/cm to 160 S/cm. The electrical conductivity of all three samples

have a dramatic decrease between 140°C to 160°C.

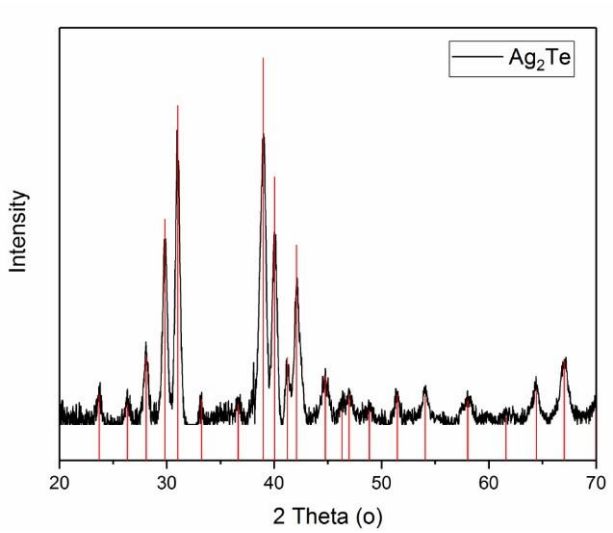

(a)

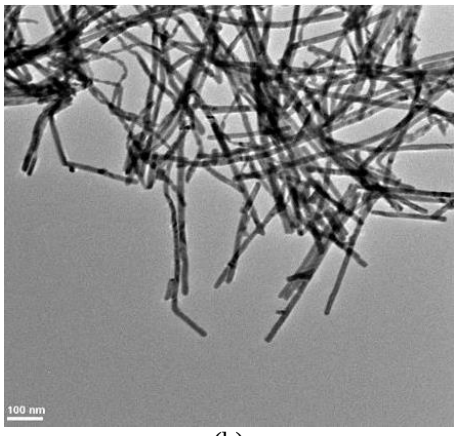

(b)

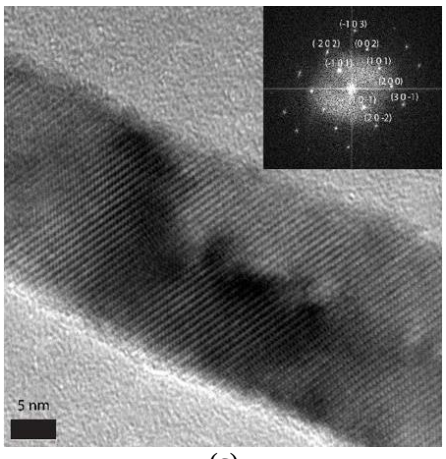

(c)

Fig. 1. (a) XRD of Ag_2Te. Red lines: standard silver telluride. (b) TEM image of Ag_2Te. (c) HRTEM of Ag_2Te (Inset: FFT of Ag_2Te).

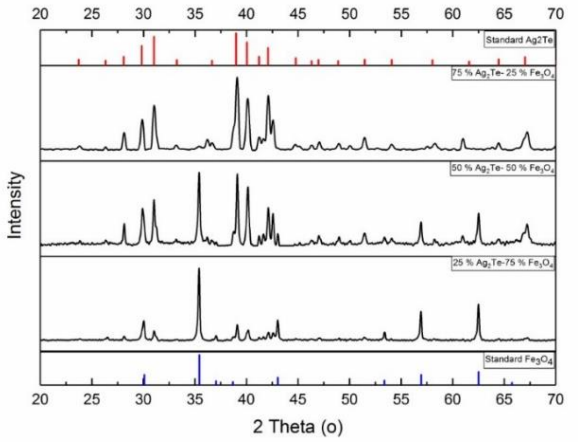

(a)

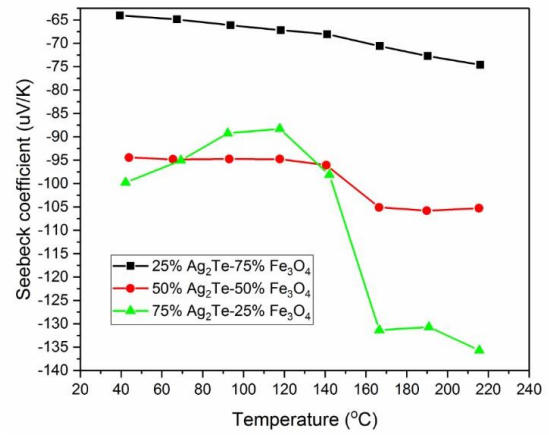

(b)

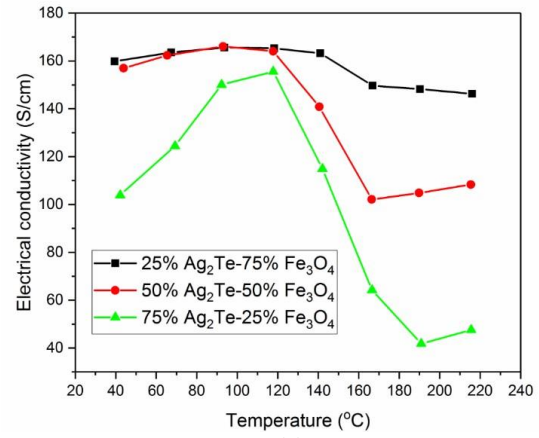

(c)

Fig. 2. (a) XRD results of Ag_2Te - Fe_3O_4 composites. All these percent numbers are weight percentages. (b) Seebeck coefficient of Ag_2Te - Fe_3O_4 composites. (c) Electrical conductivity of Ag_2Te - Fe_3O_4 composites.

As is well known, Ag_2Te changes from low-temperature monoclinic phase (α phase) to high-temperature cubic phase (β phase) at 150°C [35-36].

During phase transition from α phase to β phase, the energy band gap of Ag_2Te increases, which in turn decreases the carrier concentration (n) while the electron mobility (v) fluctuates a little bit. As a result, the electrical conductivity changes from a highly conductive state (α phase) to a poorly conductive state (β phase) based on the equation σ=nev [35, 37, 38]. This phase transition property may explain the dramatic changes in Figure 2b and 2c, especially for the sample of 75% Ag_2Te-25% Fe_3O_4. As to the $FeTe_2$, it shows a temperature-dependent reversible and reproducible switching behavior between p-type to n-type conduction [33].

Magnetite is one of the most important resources for production of iron via microwave heating because of its good coupling with microwaves and three mechanisms including Joule loss, dielectric loss, and magnetic loss would contribute to microwaves heating [39]. Thus, the magnetite is mixed with the silver telluride nanowire to increase the EM absorption of the composites. Figure 3 shows the EM absorption of the three Ag_2Te - Fe_3O_4 composite disks with different mass percentage compositions (75% Fe_3O_4-25% Ag_2Te, 50% Fe_3O_4-50% Ag_2Te, 25% Fe_3O_4-75% Ag_2Te), and the iron telluride nanodisk in X band. The measurement was performed by placing the disks in an X-band waveguide with the disk face parallel to the waveguide cross-section to ensure the same experiment condition. The input power p_0 is 0 dBm. All disks are 1.6 mm thick. The EM absorption is calculated from the measured S parameters and is given by $\left(1-\left|S_{11}\right|^2-\left|S_{21}\right|^2\right)p_0$ [40-42].

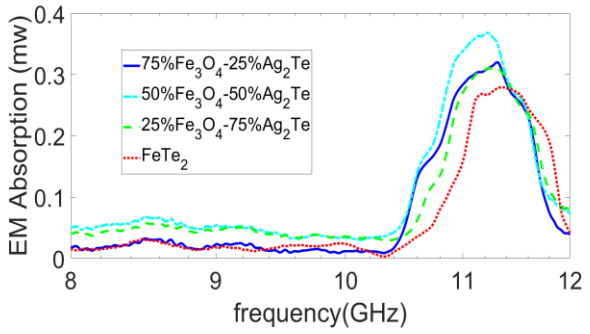

Fig. 3. EM absorption of samples in X band.

The maximum EM absorption power measured is 0.37 mW, which occurs at 11.2 GHz with the composite made of 50% Fe3O4-50% Ag2Te. This composite also shows better EM absorption performance over others in the frequency range from 8 GHz to 11.4 GHz. For the composites made of 25% Fe_3O_4-75% Ag_2Te, 75% Fe_3O_4-25% Ag_2Te, and the iron telluride, the maximum absorption power is 0.31 mW at 11.31 GHz, 0.32 mW at 11.29 GHz and 0.28 mW at 11.35 GHz, respectively. At least 30% power is absorbed by the samples at around 11 GHz. The potential sensors can absorb high-power EM radiation and convert it to heat, which results in a temperature rise given by $\Delta T = Q/C$, where Q is the amount of the heat absorbed and C is the heat capacity [43]. The temperature rise eventually leads to rapid change in electrical conductivity by α-type to β-type phase transition for Ag_2Te - Fe_3O_4 samples as shown in Fig. 2, and p-type to n-type transition in iron telluride with reversible and reproducible switching behavior [33]. A multi-physics simulation package is needed to include electromagnetic modeling of energy absorptivity of the mixtures at different frequencies, thermal modeling of temperature changes, and chemical modeling of electrical conductivity changes from α-type to β-type phase transition in silver telluride and p-type to n-type transition in iron telluride. The electromagnetic radiation driven phase transitions in Ag_2Te - Fe_3O_4 and $FeTe_2$ nano-composites can be potentially applied to develop EM sensors.

IV. CONCLUSIONS

It is shown in this work that the iron telluride and mixture composites made of silver telluride nanowire and iron oxide powder have good EM absorption in X band and exhibit rapid changes of electrical property in a certain temperature range. The composite made of 50% Fe3O4-50% Ag2Te has the maximum EM absorption power at 11.2 GHz which leads to the temperature rise. In turn, the temperature rise causes a rapid change in the electrical conductivity by α-type to β-type phase transition in the composite mixtures and p-type to n-type transition in iron telluride, which can be potentially exploited for developing EM sensors.

V. ACKNOWLEDGEMENTS

This work is supported in part by Office of Naval Research (Award number N00014-16-1-2066), in part by the IU Program of the Center for Nondestructive Evaluation at Iowa State University, and in part by China Scholarship Council.

REFERENCES

[1] G. B Sun, B. X Dong, *et al.*, "Hierarchical dendrite-like magnetic materials of Fe3O4, γ-Fe2O3, and Fe with high performance of microwave absorption," *Chemistry of Materials*, vol. 23, pp. 1587-1593, 2011.

[2] W. M. Zhu, L. Wang, *et al.*, "Electromagnetic and microwave-absorbing properties of magnetic nickel ferrite nanocrystals," *Nanoscale*, vol. 3, pp. 2862-2864, 2011.

[3] Z. Piotrowski, *et al.*, "Electromagnetic compatibility

of the military handset with hidden authorization function based on MIL-STD-461D results," *Progress in Electromagnetics Research*, vol. 4, pp. 566-570, 2008.

[4] G. Y. Slepyan, A. Boag, V. Mordachev, *et al*., "Nanoscale electromagnetic compatibility: Quantum coupling and matching in nanocircuits," *IEEE Transactions on Electromagnetic Compatibility*, vol. 57, no. 6, pp. 1645-1654, Dec. 2015.

[5] D. Sun, Q. Zou, G. Qian, *et al*., "Controlled synthesis of porous Fe3O4-decorated graphene with extraordinary electromagnetic wave absorption properties," *Acta Materialia*, vol. 61, pp. 5829-5834, 2013.

[6] V. Balchiunas, S. Baleivichius, and A. Deksnys, "Size effect of nanosecond switching in submicron coplanar structures based on amorphous semi-conductors," *Lietuvos Fizikos Rinkinys*, vol. 4, no. 405, 1991.

[7] S. Balevičius, *et al*., "Ultrafast electrical super-conducting to normal states switching in Y-Ba-Cu-O and Bi-Sr-Ca-Cu-O microstrips," *MRS Online Proceedings Library Archive*, vol. 275, pp. 1-5, 1992.

[8] T. Kikel, L. Altgilbers, *et al*., "Plasma limiters," in *AIAA Plasmadynamics and Laser Conference*, vol. 98, no. 2564, 1998.

[9] L. Altgilbers, *et al*., "Fast protector against EMP using electrical field induced resistance change in La/sub 0.67/Ca/sub 0.33/MnO/sub 3/thin films," *Pulsed Power Plasma Science*, vol. 2, pp. 1782-1785, 2001.

[10] S. Balevicius, *et al*., "Fast protector against EMP using thin epitaxial and polycrystalline manganite films," *IEEE Electron Device Letters*, vol. 32, pp. 551-553, 2011.

[11] S. Balevicius, *et al*., "EMP effects on high-T/sub c/superconducting devices," *IEEE transactions on Applied Superconductivity*, vol. 14, pp. 112-118, 2004.

[12] N. Žurauskienė, "Thin manganite films for fast fault current limiter applications," *Thin Solid Films*, vol. 515, pp. 576-579, 2006.

[13] Y. Ding, L. Zhang, *et al*., "Electromagnetic wave absorption in reduced graphene oxide functionalized with Fe3O4/Fe nanorings," *Nano Research*, vol. 9, pp. 2018-2025, 2016.

[14] X. Li, X. Yin, C. Song, *et al*., "Self‐assembly core–shell graphene‐bridged hollow MXenes spheres 3D foam with ultrahigh specific EM absorption performance," *Advanced Functional Materials*, vol. 28, no. 41, p. 1803938, Aug. 2018.

[15] M. I. Hossain, M. R. I. Faruque, and M. T. Islam, "A new design of cell phone body for the SAR reduction in the human head," *Applied Computational Electromagnetics Society Journal*, vol. 30, no. 7, pp. 792-798, July 2015.

[16] G. Wang, X. Peng, L. Yu, *et al*., "Enhanced microwave absorption of ZnO coated with Ni nanoparticles produced by atomic layer deposition," *Journal of Materials Chemistry A*, vol. 3, no. 6, pp. 2734-2740, Dec. 2015.

[17] N. O. Parchin, M. Shen, and G. F. Pedersen, "Small-size tapered slot antenna (TSA) design for use in 5G phased array applications," *Applied Computational Electromagnetics Society Journal*, vol. 32, no. 3, pp. 193-202, Mar. 2017.

[18] Y. V. Pershin and D. V. Massimiliano, "Memory effects in complex materials and nanoscale systems," *Advances in Physics*, vol. 60, pp. 145-227, 2011.

[19] A. D. Smith, K. Elgammal, F. Niklaus, *et al*., "Resistive graphene humidity sensors with rapid and direct electrical readout," *Nanoscale*, vol. 7, pp. 19099-19109, Oct. 2015.

[20] J. Yang, D. Joshua, B. Strukov, and R. S. Duncan, "Memristive devices for computing," *Nature Nanotechnology*, vol. 8, no. 13, 2013.

[21] K. Ohta, Y. Kuwayama, K. Hirose, *et al*., "Experimental determination of the electrical resistivity of iron at Earth's core conditions," *Nature*, vol. 534, pp. 95-98, June 2016.

[22] O. Sato, "Dynamic molecular crystals with switchable physical properties," *Nature Chemistry*, vol. 8, pp. 644, 2016.

[23] H. Zhao and J. Bai, "Highly sensitive piezo-resistive graphite nanoplatelet–carbon nanotube hybrids/polydimethylsilicone composites with improved conductive network construction," *ACS Applied Materials & Interfaces*, vol. 7, no. 18, pp. 9652-9659, Apr. 2015.

[24] H. Layssi, P. Ghods, A.R. Alizadeh, *et al*., "Electrical resistivity of concrete," *Concrete International*, vol. 37, no. 5, pp. 41-46, May 2015.

[25] F. Li, *et al*., "Phase-transition-dependent conductivity and thermoelectric property of silver telluride nanowires," *The Journal of Physical Chemistry C*, vol. 112, pp. 16130-16133, 2008.

[26] F. Messerschmitt, M. Kubicek, and J. L. M. Rupp, "How does moisture affect the physical property of memristance for anionic–electronic resistive switching memories?," *Advanced Functional Materials*, vol. 25, no. 32, pp. 5117-5125, July 2015.

[27] C. Guo, X. Shang, J. Li, *et al*., "A lightweight 3-D printed X-band bandpass filter based on spherical dual-mode resonators," *IEEE Microwave and Wireless Components Letters*, vol. 26, no. 8, pp. 568-570, Aug. 2016.

[28] H. Li, G. Wang, H. X. Xu, *et al*., "X-band phase-gradient metasurface for high-gain lens antenna application," *IEEE Transactions on Antennas and*

Propagation, vol. 63, no. 11, pp. 5144-5149, Nov. 2015.

[29] M. Han, *et al*., "Ti3C2 MXenes with modified surface for high-performance electromagnetic absorption and shielding in the X-band," *ACS Applied Materials & Interfaces*, vol. 8, pp. 21011-21019, 2016.

[30] J. Zhang, H. Yang, and H. Liang, "Band-notched split-ring resonators loaded monopole antenna for ultrawideband applications," *Applied Computational Electromagnetics Society Journal*, vol. 28, no. 2, pp. 137-142, Feb. 2013.

[31] A. Qin, *et al*., "Silver telluride nanotubes prepared by the hydrothermal method," *Inorganic Chemistry*, vol. 46, pp. 7403-7409, 2007.

[32] H. Yang, *et al*., "Composition modulation of Ag2Te nanowires for tunable electrical and thermal properties," *Nano Letters*, vol. 14, pp. 5398-5404, 2014.

[33] W. Zheng, *et al*., "Solution-phase synthesized iron telluride nanostructures with controllable thermally triggered p-type to n-type transition," *Nanoscale*, vol. 10, pp. 20664-20670, 2018.

[34] J. H. Lee, J. H. Kim, and S. S. Kim, "CuO–TiO2 p–n core–shell nanowires: Sensing mechanism and p/n sensing-type transition," *Applied Surface Science*, vol. 448, pp. 489-497, Aug. 2018.

[35] S. Aliev, Z. Agaev, and E. Zul'figarov, "Charge transport in silver chalcogenides in the region of phase transition," *Semiconductors*, vol. 41, pp. 1027-1032, 2007.

[36] Y. Pei, N. A. Heinz, and G. J. Snyder, "Alloying to increase the band gap for improving thermoelectric properties of Ag2Te," *Journal of Materials Chemistry*, vol. 21, pp. 18256-18260, 2011.

[37] S. Aliev, "Hysteresis in Ag2Te near and within the phase transition region," *Semiconductors*, vol. 38, pp. 796-799, 2004.

[38] F. Aliev, "Phase transition of Ag-Enriched Ag2Te," *Inorganic Materials*, vol. 38, pp. 995-997, 2002.

[39] A. Amini, *et al*., "Effect of particle size and apparent density on the initial stages of temperature increase during the microwave heating of Fe3O4," *Powder Technology*, vol. 338, pp. 101-109, 2018.

[40] R. S. Rao, *Microwave Engineering*. PHI Learning Pvt. Ltd, 2015.

[41] S. Luo, Y. Li, Y. Xia, *et al*., "A low mutual coupling antenna array with gain enhancement using metamaterial loading and neutralization line structure," *Applied Computational Electromagnetics Society Journal*, vol. 34, no. 3, pp. 411-418, Mar. 2019.

[42] P. Ferrazzoli, L. Guerriero, and D. Solimini, "Numerical model of microwave backscattering and emission from terrain covered with vegetation," *Applied Computational Electromagnetics Society Journal*, vol. 6, no. 1, pp. 175-191, June 1991.

[43] W. J. Parker, *et al*., "Flash method of determining thermal diffusivity, heat capacity, and thermal conductivity," *Journal of Applied Physics*, vol. 32, pp. 1679-1684, 1961.